Cell. Mol. Life Sci. (2016) 73:3733–3744
DOI 10.1007/s00018-016-2215-0

Cellular and Molecular Life Sciences

ORIGINAL ARTICLE

Ebola virus encodes a miR-155 analog to regulate importin-α5 expression

Yuanwu Liu[1] · Jing Sun[1] · Hongwen Zhang[2] · Mingming Wang[1] · George Fu Gao[3] · Xiangdong Li[1]

Received: 10 December 2015 / Revised: 31 March 2016 / Accepted: 1 April 2016 / Published online: 19 April 2016

Abstract The 2014 outbreak of Ebola virus caused more than 10,000 human deaths. Current knowledge of suitable drugs, clinical diagnostic biomarkers and molecular mechanisms of Ebola virus infection is either absent or insufficient. By screening stem-loop structures from the viral genomes of four virulence species, we identified a novel, putative viral microRNA precursor that is specifically expressed by the Ebola virus. The sequence of the microRNA precursor was further confirmed by mining the existing RNA-Seq database. Two putative mature microRNAs were predicted and subsequently validated in human cell lines. Combined with this prediction of the microRNA target, we identified importin-α5, which is a key regulator of interferon signaling following Ebola virus infection, as one putative target. We speculate that this microRNA could facilitate the evasion of the host immune system by the virus. Moreover, this microRNA might be a potential clinical therapeutic target or a diagnostic biomarker for Ebola virus.

Keywords Ebola virus · MicroRNA · Host immune system · Interferon signal pathway

Introduction

Ebola virus disease (EVD) was first identified in 1976 during simultaneous outbreaks in Sudan and the Democratic Republic of Congo, with patients exhibiting impaired kidney and liver function as the main symptoms [1, 2]. The EVD pathogen is an enveloped, negative-sense RNA virus, belonging to *Filoviridae* family, genus *Ebolavirus*. Four species in this genus have been identified as pathogens that can cause disease in human and non-human primates: *Zaire ebolavirus* (EBOV), *Sudan ebolavirus* (SUDV), *Tai Forest ebolavirus* (TAFV) and *Bundibugyo ebolavirus* (BDBV) [3]. Due to differences between species, the fatality rate caused by EVD ranges from 25 to 90 % [4]. The recent West African outbreak of EBOV caused 28,575 reported cases of suspected infection and 11,313 deaths according to the World Health Organization situation report (http://apps.who.int/ebola/current-situation). However, no licensed antiviral vaccine or effective treatments is currently available for clinical application [5–12].

MicroRNA (miRNA) is a class of small, non-coding RNAs that range in length from 19 to 24 nt and which regulate target gene expression at a posttranscriptional level through degradation or translational suppression [13–15]. The use of available miRNA databases has enabled thousands of miRNAs to be identified in mammalian and plant cells, but few miRNAs have been found in viral genomes, especially in those of RNA viruses [16]. Despite the initial lack of acceptance regarding the existence of RNA virus-derived miRNA [17, 18], a growing body of evidence, based on mature sequence prediction and

Electronic supplementary material The online version of this article (doi:10.1007/s00018-016-2215-0) contains supplementary material, which is available to authorized users.

✉ Xiangdong Li
xiangdongli@cau.edu.cn

[1] State Key Laboratory of Agrobiotechnology, College of Biological Sciences, China Agricultural University, No. 2, Yuanmingyuan West Rd, 100193 Beijing, China

[2] Department of General Surgery, The 306th Hospital of PLA, Beijing, China

[3] CAS Key Laboratory of Pathogenic Microbiology and Immunology, Institute of Microbiology, Chinese Academy of Sciences, Beijing, China

experimental validation, confirms these earlier reports. More importantly, mechanisms for RNA virus-derived miRNA processing have been elucidated [19]. Recently, miRNAs encoded by RNA viruses have been identified, including those encoded by human immunodeficiency virus [20], West Nile virus [21], bovine leukemia virus [22, 23], Dengue virus [24–26] and hepatitis A virus [27].

Two independent research groups have recently predicted Ebola virus-encoded miRNAs [28, 29]. In their respective studies, Teng et al. [28] and Liang et al. [29] analyzed putative miRNAs from consensus sequences of EBOV and SUDV or those from the 2014 EBOV outbreak. In contrast, in our study we focused on EBOV-specific miRNAs and examined why EBOV, among the pathogens in genus *Ebolavirus* that can cause disease in human and non-human primates, causes the highest death rate in humans. To answer this question, stem-loop structures specific to EBOV were selected by screening the genomes of these four *Ebolavirus* species and predicting their potential miRNA coding regions. MiRNA prediction and target validation revealed an hsa-miR-155-5p analog generated only by EBOV, named Zebov-miR-1-5p, which alters importin-α5 (KPNA1) expression, possibly causing dysfunction of the interferon (IFN) signaling pathway and increasing the mortality of infected patients.

Materials and methods

Comparison and sequence analysis of the *ebolavirus* genome

The *ebolavirus* genome sequence was compared to genome sequences in the online NIAID Virus Pathogen Database and Analysis Resource (ViPR) (website: http://www.viprbrc.org). A phylogenetic tree was generated automatically based on data from outbreak species of the *ebolavirus* recorded from 1976 to 2014 in the ViPR online resources. For genome sequence analysis, we downloaded one EBOV genome, KM519951.1, from the National Center for Biotechnology Information (http://www.ncbi.nlm.nih.gov/).

Bioinformatics prediction of the miRNAs and the target gene

To identify the putative miRNA precursor sequences in the virus genome we used miRNAFold (http://evryrna.ibisc.univ-evry.fr/miRNAFold) [30] to predict the stem-loop structure in the virus genome by parameters following 90 % of the verified features and *Homo Sapiens* species. To narrow down the results on prediction, we used another two web-based software tools, MiPred (http://www.bioinf.seu.edu.cn/miRNA) [31] and miRD (http://mcg.ustc.edu.cn/rpg/mird) [32], to screen putative miRNA precursors (pre-miRNA). For the prediction of mature miRNA sequences, we used Mature Bayes tools (http://mirna.imbb.forth.gr/MatureBayes.html) [33] by default parameters. To view the secondary structure of miRNA precursors we simulated the two- and three-dimensional (2D and 3D, respectively) structures by RNAfold (http://rna.tbi.univie.ac.at/) and RNAComposer (http://rnacomposer.cs.put.poznan.pl/) respectively [34, 35].

EBOV RNA-Seq data analysis from infected patients

We randomly downloaded four independent sets of RNA-Seq raw data (SRX733663, SRX733662, SRX674130 and SRX674148) deposited in the NCBI project (Accession No. PRJNA257197) and mapped into the EBOV genome by the web-based NGS platform Galaxy (https://usegalaxy.org/) [36–38]. Mapping results were checked using Tablet software [39, 40]. The EBOV genome structure for RNA-Seq data comparison was generated from the UCSC genome browser (http://genome.ucsc.edu) [41].

EBOV miRNA target prediction and function analysis

EBOV miRNA target genes were predicted using TargetScan Human Custom web-based methods (http://www.targetscan.org) [42]. Target genes were analyzed further by molecular function, biological process and pathway analysis using PANTHER (http://www.pantherdb.org/) [43]. The target gene net regulation map was constructed using ConsensusPathDB-human integrated interaction networks (http://cpdb.molgen.mpg.de/) [44, 45].

Cells, plasmids and reagents

HEK293T and Hela cells (American Type Culture Collection, Manassas, VA) were cultured in Dulbecco's Modified Eagle's Medium–high glucose (Sigma, St. Louis, MO) supplemented with 10 % fetal bovine serum (HyClone; Thermo Fisher Scientific, Waltham, MA), at 37 °C in an incubator with 5 % CO_2. The eukaryotic expression plasmid, pmCherry-C1, was generated from pEGFP-N1 by substituting *EGFP* (*Enhanced Green Fluorescent Protein*) with *mCherry*. Predicted EBOV miRNA precursor sequences were direct synthesized (Sangon Biotech, Shanghai, China) and ligated into 5′- or 3′-untranslated regions of *mCherry*. EBOV miRNA expression plasmids and Zebov-miR-1-5p miRNA mimics (GenePhama, Shanghai, China) were transfected by lipofectamine 3000 (Invitrogen, Carlsbad, CA) following

the manufacturer's instructions. The luciferase reporter vector psiCHEK2 (Promega, Madison, WI) was used to identify putative targets of miRNA, target sequences, and positive control sequences were directly synthesized (Table S1) and inserted following the luciferase reporter gene. All of the constructs generated were confirmed by sequencing using universal primers.

RNA isolation and quantitative reverse transcription-PCR

Total RNA and miRNA were extracted from the cultured cells using the TRIzol reagent and a miRNA isolation kit (CWBio, Beijing, China) according to the manufacturer's instructions. MiRNA reverse transcription (RT) was performed following stem-loop methods to quantify the miRNA [46]. Briefly, 2 μg of total RNA was reverse-transcribed to cDNA using the M-MLV reverse transcriptase (Takara, Tokyo, Japan) under the following reaction conditions: 16 °C for 30 min, 42 °C for 30 min, and 85 °C for 5 min. Real-time PCR was performed using a Roche real-time PCR kit on a LightCycler480 PCR cycler (Roche Diagnostics, Risch-Rotkreuz, Switzerland). The reactions were incubated in a 96-well plate at 95 °C for 10 min, followed by 40 cycles of 95 °C for 10 s, 60 °C for 10 s and 72 °C 10 s. The PCR products were detected by 2 % agarose gel electrophoresis. All of the reactions were run in triplicate.

Luciferase reporter assay

A dual luciferase reporter assay using the sensor plasmid psiCHEK2 was performed in HEK293T cells. Briefly, HEK293T cells were seeded at a density of approximately 1×10^6 cells per well in a 24-well plate 1 day prior to transfection. On day following seeding, 100 ng of psi-CHEK2-TS was co-transfected with 20 pmol of chemically synthesized miRNA mimics (GenePharma) with Lipofectamine 3000. The Firefly and Renilla luciferase activities were evaluated simultaneously 48 h post-transfection using the Dual Luciferase Assay kit (Galen, Beijing, China) according to the manufacturer's protocol. Relative luciferase activity was normalized as the ratio of Firefly to Renilla luciferase activity. The transfections were performed independently in triplicate.

Western blot analysis

The total protein of the cell extracts was quantified using the BCA protein assay kit (TianGen, Beijing, China) according to the manufacturer's instructions. Briefly, 30 μg of total protein was resolved on 12 % sodium dodecyl sulfate-polyacrylamide gel electrophoresis gels and transferred onto PVDF membranes (Millipore, Billerica, MA), followed by blocking with 2 % non-fat milk at room temperature for 2 h. Membranes were probed with the importin-α5 primary antibodies (Sangon) at 1:1000 dilution overnight at 4 °C, followed by incubation with the 1:5000 dilution of anti-mouse HRP-conjugated secondary antibodies (ZSGB-Bio, Beijing, China) at room temperature for 1 h. Protein signals were visualized using the Pierce ECL Western Blotting Substrate (Thermo Fisher Scientific) according to the manufacturer's protocol. The western blot results were quantified using Image J software (http://rsb.info.nih.gov/ij/).

Statistical analysis

Data were presented as mean ± standard error of the mean. Values from three independent experiments were analyzed by the two-tailed Student's *t* test (GraphPad Software, Inc., La Jolla, CA). Statistical significance was set at $P < 0.05$.

Results

EBOV genome analysis and putative miRNA prediction

The genus *Ebolavirus* contains five species. To investigate the distance between these species using genome nucleotides, we selected the outbreak species and constructed a phylogenetic tree (Fig. 1a). As this tree enabled us to clearly separate the five *Ebolavirus* species, we concluded that EBOV has a specific genome nucleotide that is correlated to functions. Based on this result, we carried out a bioinformatics analysis to further investigate the specific characteristics of the EBOV genome (Fig. 1b). The primary analysis yielded 24 sequences with potential stem-loop structures [Electronic Supplementary Material (ESM) Table S2]. To narrow down candidate structures, we used two miRNA coding stem-loop structure identification programs that identified, with relatively high prediction confidence, one putative miRNA coding precursor (ESM Fig. S1a), which was named Zebov-pre-miR-1 (Table 1). The 2D and 3D structures of Zebov-pre-miR-1 were also predicted (ESM Fig. S1b, c); these results indicate a very stable secondary structure. We then predicted two putative mature miRNAs, each with a lengths of 22 nt, which were named Zebov-miR-1-5p and Zebov-miR-1-3p, respectively (Table 1). Using computational approaches, we identified one unique putative pre-miRNA and two putative mature miRNAs from the EBOV genome.

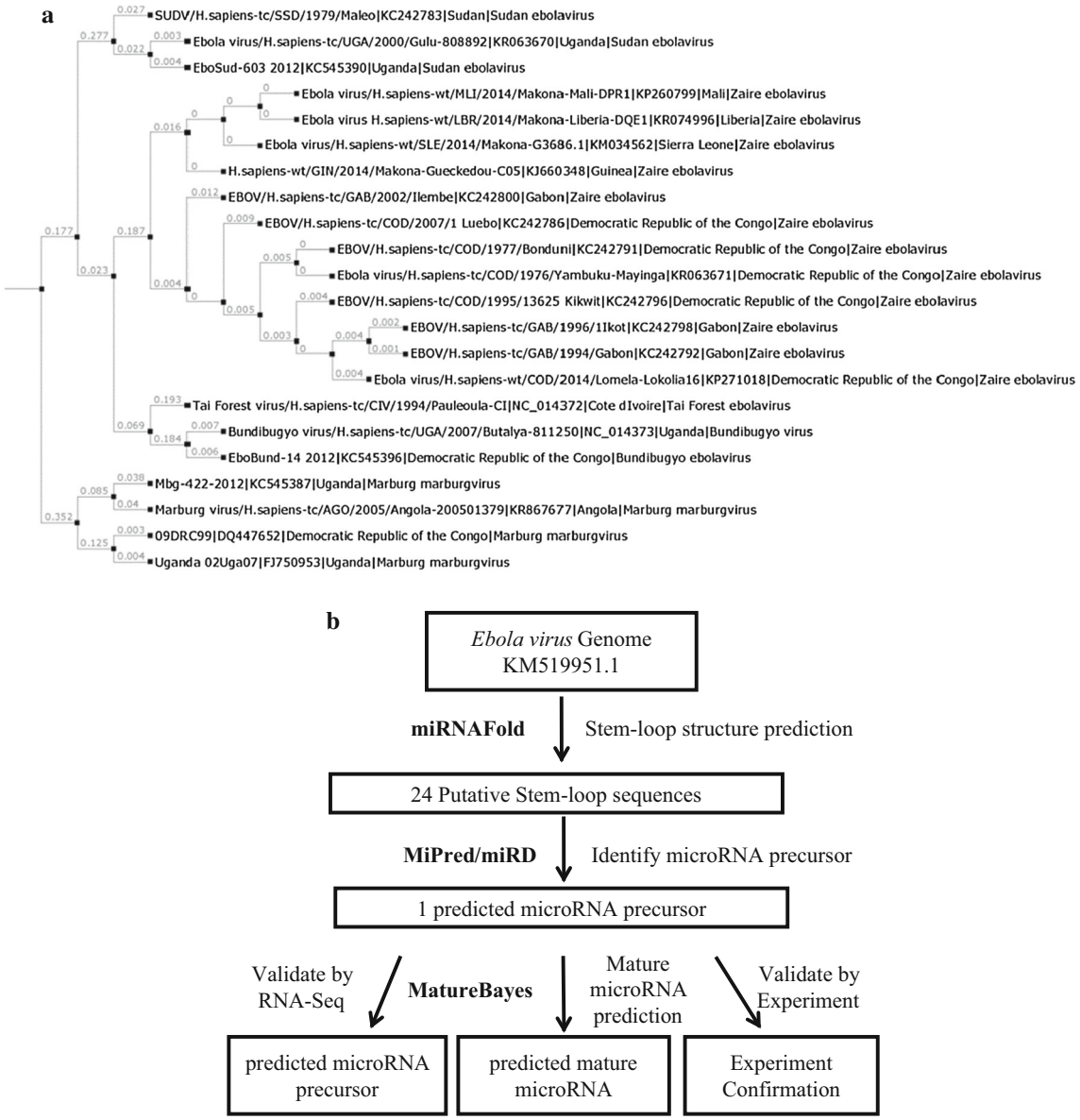

Fig. 1 Phylogenetic analysis of outbreak species of *ebolavirus* from 1976 to 2014 and workflow of *Zaire ebolavirus* (*EBOV*) microRNA (miRNA) prediction and validation. **a** Phylogenetic analysis for *ebolavirus*. A total of 22 strains of EBOV associated with Ebola virus disease outbreaks from 1976 to 2014 were identified and used in the phylogenetic analysis for this genome. *Numbers on branches* Relative genetic distance between strains. **b** Workflow of EBOV-encoded miRNA prediction. EBOV genomes were first screened for stem-loop structure by miRNAFold. They were then screened for miRNA-specific structures using MiPred and miRD to identify the miRNA precursor. RNA-Seq data was used to validate the miRNA precursor, and the mature miRNA was predicted by the Mature Bayes tool and finally validated by stem-loop reverse transcription-PCR

Table 1 Predicted miRNA precursor and mature sequences of *Zaire ebolavirus* (EBOV)

Name	Predicted sequences	Length (nt)	Genome position
Zebov-pre-miR-1	UGCUAAACUAAUGAUGAAGAUUAAUGCG GAGGUCUGAUAAGAAUAAACCUUAUUA UUCAGAUUAGGCCCCAAGAGGCAUUCU UCAUCUCCUUUUAGCA	98	9869–9966
Zebov-miR-1-5p	AUUAAUGCGGAGGUCUGAUAAG	22	9889–9910
Zebov-miR-1-3p	AGAUUAGGCCCCAAGAGGCAUU	22	9928–9949

Table 2 Predicted top target genes of Zebov-miR-1-5p

Target gene	Gene name	Conserved sites			
		Total	8mer	7mer-m8	7mer-1A
TRPS1	Trichorhinophalangeal syndrome I	4	2	0	2
TSHZ3	Teashirt zinc finger homeobox 3	3	1	2	0
BAG5	BCL2-associated athanogene 5	2	2	0	0
FGF7	Fibroblast growth factor 7 (keratinocyte growth factor)	2	2	0	0
LAMP2	Lysosomal-associated membrane protein 2	2	2	0	0
NFIB	Nuclear factor I/B	2	2	0	0
KPNA1	Karyopherin alpha 1 (importin alpha 5)	3	1	1	1
E2F2	E2F transcription factor 2	2	1	1	0
JARID2	Jumonji, AT rich interactive domain 2	2	1	1	0
KLF3	Kruppel-like factor 3 (basic)	2	1	1	0
SMAD2	SMAD family member 2	2	1	1	0
BCL2	B-cell CLL/lymphoma 2	2	1	0	1
CREB1	cAMP responsive element binding protein 1	2	1	0	1
NAV3	Neuron navigator 3	2	1	0	1
VTI1A	Vesicle transport through interaction with t-SNAREs homolog 1A (yeast)	2	1	0	1
ZFAND5	Zinc finger, AN1-type domain 5	2	1	0	1
ZFHX4	Zinc finger homeobox 4	2	1	0	1
PPP1R12B	Protein phosphatase 1, regulatory (inhibitor) subunit 12B	3	0	1	2

EBOV miRNA precursor and mature sequence validation

Predicted results were compared against published RNA-Seq data from sera of patients infected by the 2014 outbreak EBOV [47]. This comparison revealed a short sequence enrichment near the predicted position. Mapping results indicated that a small fragment near the predicted position was enriched in all selected samples (Fig. 2a). The exact sequence of the indicated region is shown in Fig. 2b and can be seen to be nearly identical to the predicted miRNA precursor sequence. To address the lack of miRNA sequencing data, as well as scarcity of biosafety level 4 laboratories, we used a plasmid-derived miRNA expression system to identify the mature miRNA sequence. The Zebov-pre-miR-1 sequence together with 100-bp native flanking sequences were inserted into the miRNA expression plasmid (Fig. 3a). After transfection of the mammalian cell lines, we observed a strong fluorescent signal (Fig. 3b), which indicates that the Zebov-pre-miR-1 precursor sequence was expressed properly. Stem-loop RT-PCR analysis of the transfected cells and negative controls (transfection with plasmids only) revealed that Zebov-miR-1-5p and Zebov-miR-1-3p were expressed in the former (Fig. 3c).

Most miRNA precursors were found to be located downstream of the host genes, while the predicted miRNA precursor is located upstream of the virus VP24 gene. To test for the effects on processing by a miRNA precursor located upstream of genes, we inserted Zebov-pre-miR-1 and its native flanking sequences at the 5′-UTR of the mCherry gene (Fig. 3a). After transfection and miRNA isolation, the mature sequences of Zebov-miR-1-5p and Zebov-miR-1-3p were determined (Fig. 3c). Together, these results indicate that the EBOV genome can generate one miRNA precursor that develops into two mature miRNAs.

Prediction and function analysis of EBOV miRNA targets

In mammalian cells, miRNAs usually bind to the 3′-UTR of target genes by six to eight nucleotides at the 5′ end (the seed region). Seed region sequences were selected to identify the gene targets of EBOV miRNAs, using TargetScan. The predicted target genes that contained at least two conserved target sites are shown in Table 2. Since all target genes predicted for Zebov-miR-1-3p were found to contain only one conserved binding site, these target genes do not fit the pre-specified criteria for further study. The subsequent functional analysis focused primarily on the target genes from Zebov-miR-1-5p. To identify putative functions of the novel miRNA, we analyzed the biological process and the pathway of target gene enrichment using

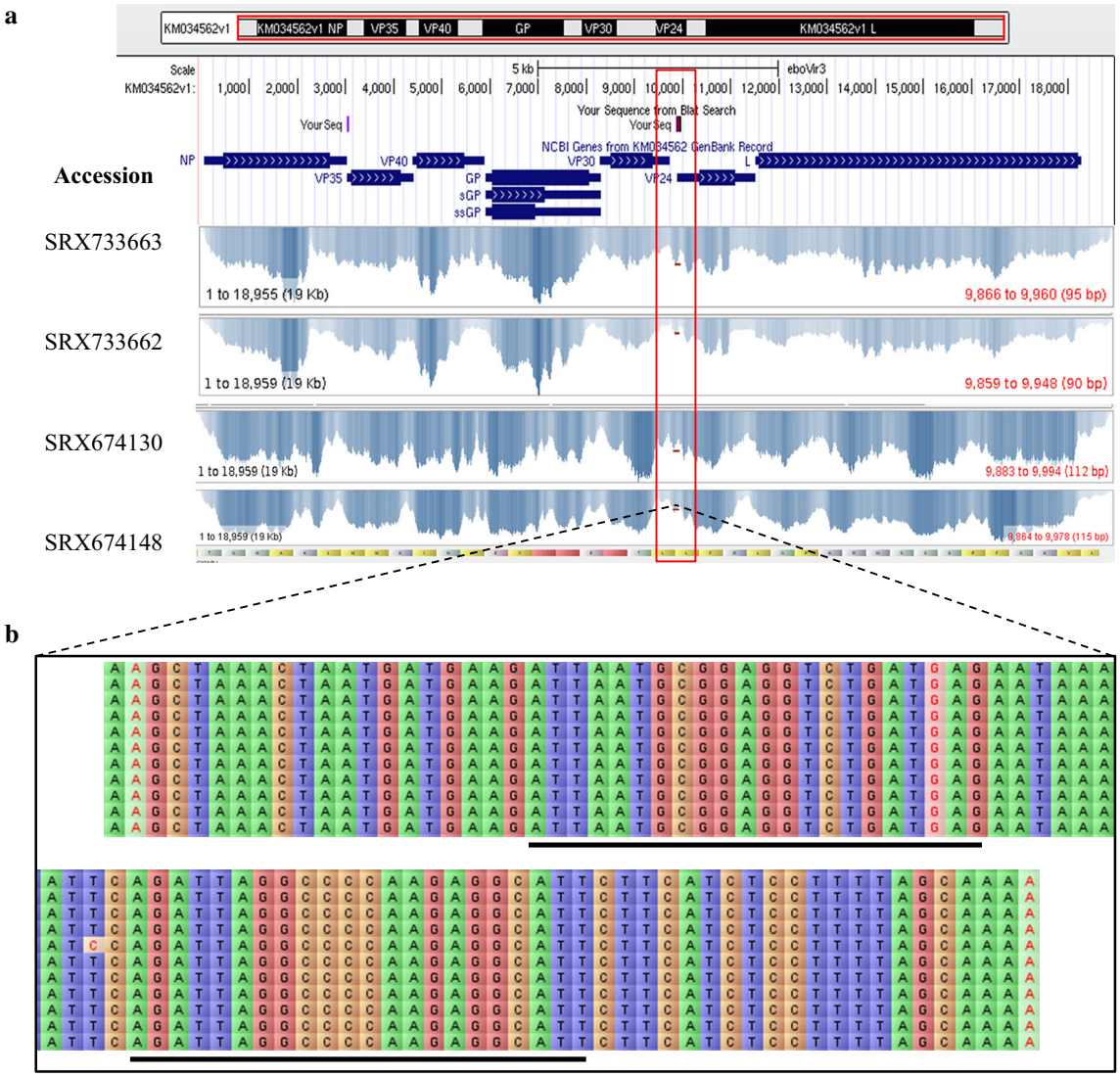

Fig. 2 RNA-Seq data mapping to EBOV genome. **a** Blood samples from EBOV-infected patient for RNA-Seq data mapping to EBOV genome. All patient RNA-Seq sequences were assembled and mapped to the EBOV genome; the overview of the mapping results was obtained by Tablet. *Red vertical frame* indicates that all patient RNA-Seq data contain a sequencing read enrichment region at the predicted miRNA coding position. **b** Expanded view of the mapping sequences around the miRNA precursor position; the sequence in RNA-Seq was identical to the predicted sequence. *Black line* indicates the mature miRNA sequence in RNA-Seq reads data

the classification methods shown in ESM Fig. S2. Based on function annotation results, >50 % of target genes have binding functions and participate in gene regulation, suggesting the importance of target genes which contain DNA and protein-binding functions. Interestingly, the identified miRNA target gene is similar to hsa-miR-155-5p. We then compared Zebov-miR-1-5p with hsa-miR-155-5p using the RNAhybrid tool (Fig. 4a); the results of this analysis imply that Zebov-miR-1-5p has similar functions to hsa-miR-155-5p. To further analyze target gene function, we subjected all target genes to interaction network analyses (Fig. 4b), which resulted in the identification of two genes, each containing two target sites, namely, importin-α5 protein and interleukin 1 receptor accessory protein (IL1RAP) (Fig. 5a), which may participate in viral infection through their binding functions. Importin-α5 is a nuclear transport protein that interacts with virus VP24 protein to inhibit STAT1 accumulation in both nuclear and IFN signaling pathways [48–51]. Through the initiation of signaling events that result in activation of interleukin 1 response genes, the IL1RAP gene is a necessary part of the interleukin 1 receptor complex [52]. Together, these results strongly suggest that EBOV self-generates miRNAs to enhance its infectivity. This hypothesis is supported by the results of the dual-luciferase reporter assay, which demonstrated significantly reduced activity in cells co-

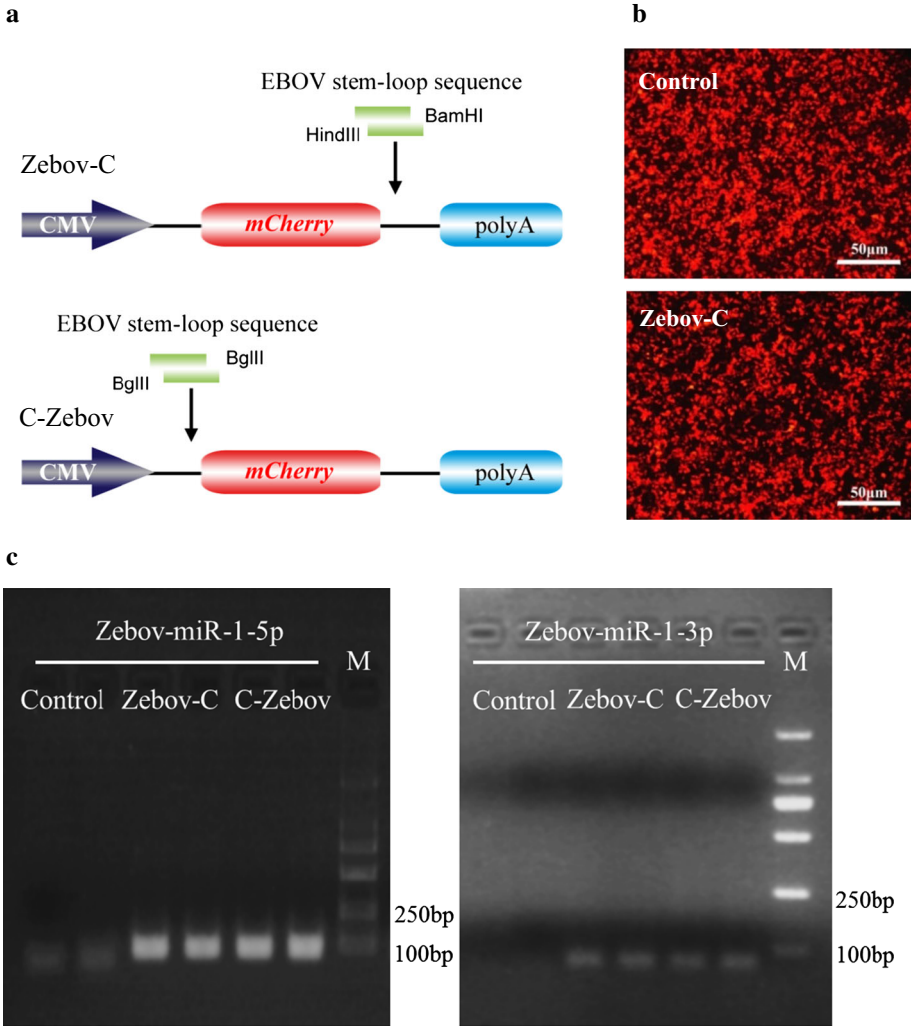

Fig. 3 Identification of mature miRNA in EBOV. **a** Construction strategy for miRNA expression plasmids, EBOV precursor sequence and its 100-bp flanking sequences inserted into the 3′-untranslated region (UTR) or 5′-UTR of mCherry. **b** The expression level and transfection efficiency in HEK293T cell lines were checked by fluorescence microscopy 24 h after transfection. **c** Two mature EBOV coding miRNA sequences were detected separately by RT-PCR, and the products were detected by 2 % agarose gel electrophoresis

transfected with Zebov-miR-1-5p and the second target site of importin-α5 gene reporter plasmid (Fig. 5b), as well as regulation of endogenous importin-α5 protein levels by Zebov-miR-1-5p (Fig. 5c). All of the data together suggest that Zebov-miR-1-5p suppresses the expression of importin-α5 protein, which in turn influences the virulence of EBOV. Overall, these results suggest that the EBOV encoded miRNAs are functionally activated.

Discussion

In the recent years EBOV has spread wildly in West Africa, especially in Sierra Leone, Liberia and Guinea [53]. The average death rate during this historic outbreak ranged from 60 to 90 % [54]. Due to the high risk in working with this virus, little fundamental progress has been made in identifying target chemicals to prevent its spread. Our results indicate that EBOV genomes can specifically encode miRNAs and that these novel miRNAs may explain the high pathogenicity of the virus. Previous studies on the ability of EBOV to evade immune surveillance focused on the functions of various proteins, such as VP35 and VP24 [48–51, 55]. Our results indicate that miRNA encoded at the 5′-UTR of the VP24 gene downregulates importin-α5 protein at the post-transcriptional level. The effect of this decrease in combination with VP24 protein binding to importin-α5 might enhance the blockage efficiency for the IFN signal. Interestingly, the 5′-UTR of VP24 has previously been reported to contain a stem-loop structure that may participate in transcription initiation, and this stem-loop structure matches our prediction [56, 57]. Taken together, these results expand our present understanding of secondary structure functions in viral genomes.

In agreement with the results of Liang et al. [29] and Teng et al. [28], we also observed miRNA produced by EBOV. However, we identified an EBOV-specific miRNA, while Liang et al. [29] identified two common miRNAs in

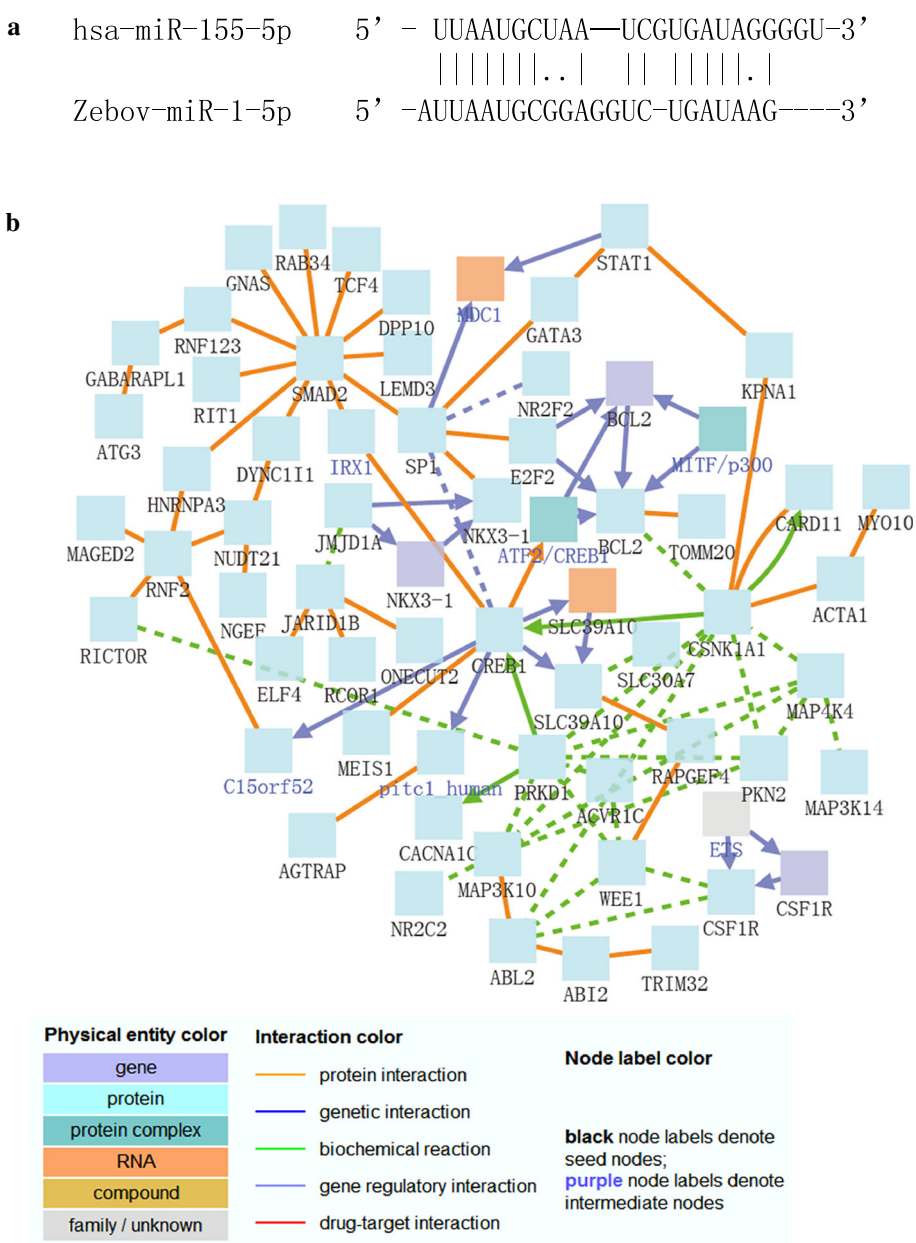

Fig. 4 EBOV miRNA target gene regulation network. **a** Zebov-miR-1-5p was compared to the human miR-155-5p mature sequence and aligned at the seed region. **b** The Zebov-miR-5p putative target gene regulation network analysis for Zebov-miR-1-5p putative function prediction

SUDV and EBOV, and Teng et al. [28] analyzed only the 2014 outbreak isolate of EBOV. In our study, we identified an EBOV miRNA present in both the 2014 outbreak and the 1976 outbreak strains. One possible explanation for the discrepancy between our data and those from these two previous studies is the difference in criteria and threshold applied for miRNA prediction. More importantly, by mining the sequences derived from EBOV-infected human sera [47], we found that the EBOV miRNA precursor sequence does exist in the region which we predicted.

Previous studies reported that EBOV infects various cell types in human and non-human primates, including dendritic cells and macrophages [58, 59]. These immune cells belong to the innate immune system and should secrete cytokines, as well as function as antigen-presenting cells and activate T cells to clear the blood of the invading pathogen. However, EBOV proteins delay maturation of these cells and weaken cytokine signal transduction by inhibiting importin function. The EBOV-encoded protein VP24 can bind to importin-α5 (KPNA1), importins-α6 (KPNA5) and importin-α7 (KPNA6), thereby sequestering importins and evading innate responses [49–51, 60]. Recent evidence in an importin-α7 knockout mouse suggests that this importin is not critical for infection in the EBOV mouse model [61]. These results further highlight importin-α5 as a key player in EBOV pathogenicity. In

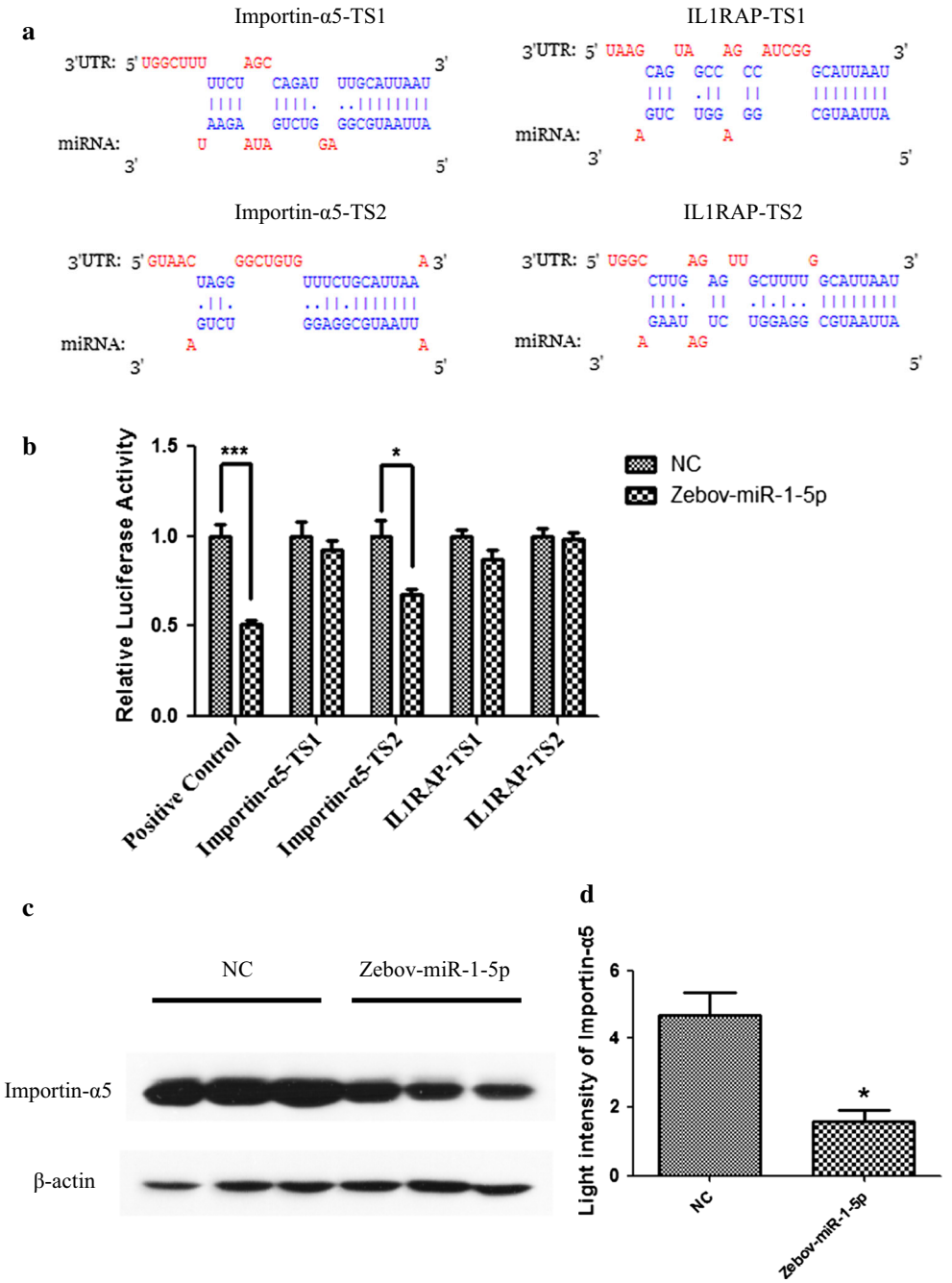

Fig. 5 EBOV miRNA target gene validation. **a** Two target sites (*TS*) of Zebov-miR-1-5p, importin-α5 (*KPNA1*) and interleukin 1 receptor accessory protei (*IL1RAP*), were predicted by TargetScan. **b** Luciferase reporter assay predicted four target sites. HEK293T cells were transfected with reporter plasmids and virus encoding miRNAs, and relative luciferase activity was expressed as the ratio of firefly to Renilla luciferase activity ($n = 5$). **c**, **d** Western-blot results of Zebov-miR-1-5p target endogenous KPNA1 protein expression level in Hela cells (**c**) and quantification of western blot results (**d**). Hela cells were transfected with 30 μM negative control (*NC*) or Zebov-miR-1-5p, total protein was extracted 48 h later to measure importin-α5 protein level; the expression of β-actin was used as an internal control. Significant at: $^{*}P < 0.05$, $^{***}P < 0.001$

addition, our results indicate that EBOV targets importin-α5 through miRNAs. Taken together, the synergetic effects of VP24 and the novel miR-155 analog may explain the higher motility rate caused by EBOV compared to other viral species.

Our analysis revealed that the predicted target gene for Zebov-miR-1-5p is nearly the same as the endogenous hsa-miR-155-5p, suggesting that during viral infection, the predicted miRNA of EBOV elicits similar responses as those of the endogenous miR-155. As observed in host

cells post-infection, miR-155 is a primary upregulated micRNAs [62–66]. Other viruses also encode functional homologs of hsa-miR-155-5p, including Kaposi's sarcoma-associated herpesvirus [67] and Marek's disease virus [68–70]. In EBOV infection, predicted miRNAs may also participate in immunity regulation by producing miR-155 analogs. Previous work on the functions of miR-155 focused on the promotion of inflammation by SOCS1, which is a repressor of type I IFN signaling [71]. More recently, Hu et al. reported that not only endogenous miR-155 but also herpes virus-encoded miR-155 orthologs could inhibit IFN-β production through its target protein-coding region (TLR3) [72].

The copy number and target genes of the mature miRNA Zebov-miR-1-3p are lower and fewer, respectively than those of the Zebov-miR-1-5p; as such functional studies of Zebov-miR-1-3p is needed. There have been reports that virus-encoded miRNA may serve as a self-repressive element that regulates virus replication [25]. We speculate that Zebov-miR-1-3p targets viral genomic RNA or the host long non-coding RNAs, rather than the 3′-UTR region of a specific gene. For Zebov-miR-1-5p also, a functional study with the real EBOV is still needed. The molecular mechanisms of all reported EBOV miRNAs on its virulence definitely need further investigation, not only in functional studies of EBOV miRNA under biosafety level 4 laboratory conditions, but also in clinical investigations on EBOV-infected human samples.

In summary, we identified two putative EBOV-encoded miRNAs, one of which is similar to the endogenous has-miR-155-5p and which functionally targets importin-α5. Together with previous reports [28, 29], these findings broaden our understanding of the virulence of EBOV and may provide a new insight for future therapeutic strategy against EVD.

Acknowledgments This work was supported by grants from the National Science and Technology Major Project (2013ZX10004608), Natural Science Foundation of China (NSFC31071316 and NSFC81261130024), National Science and Technology Major Project (2012AA020601), Ministry of Science/Technology (2009CB941701), State Key Laboratory of Agrobiotechnology Grants (2015SKLAB6-13) and the CAU Scientific Fund (No. 2012YJ034).

Compliance with ethical standards

Conflict of interest None.

References

1. Report of a WHO/International Study Team (1978) Ebola haemorrhagic fever in Sudan (1976). Report of a WHO/International Study Team. Bull World Health Organ 56(2):247–270
2. Colebunders R, Borchert M (2000) Ebola haemorrhagic fever—a review. J Infect 40(1):16–20
3. Kuhn JH, Bao Y, Bavari S, Becker S, Bradfute S, Brister JR, Bukreyev AA, Cai Y, Chandran K, Davey RA et al (2013) Virus nomenclature below the species level: a standardized nomenclature for laboratory animal-adapted strains and variants of viruses assigned to the family Filoviridae. Arch Virol 158(6):1425–1432
4. Ma DY, Suthar MS (2015) Mechanisms of innate immune evasion in re-emerging RNA viruses. Curr Opin Virol 12:26–37
5. Zhu FC, Hou LH, Li JX, Wu SP, Liu P, Zhang GR, Hu YM, Meng FY, Xu JJ, Tang R et al (2015) Safety and immunogenicity of a novel recombinant adenovirus type-5 vector-based Ebola vaccine in healthy adults in China: preliminary report of a randomised, double-blind, placebo-controlled, phase 1 trial. Lancet 385(9984):2272–2279
6. Marzi A, Robertson SJ, Haddock E, Feldmann F, Hanley PW, Scott DP, Strong JE, Kobinger G, Best SM, Feldmann H (2015) Ebola vaccine. VSV-EBOV rapidly protects macaques against infection with the 2014/15 Ebola virus outbreak strain. Science 349(6249):739–742
7. Lai L, Davey R, Beck A, Xu Y, Suffredini AF, Palmore T, Kabbani S, Rogers S, Kobinger G, Alimonti J et al (2015) Emergency postexposure vaccination with vesicular stomatitis virus-vectored Ebola vaccine after needlestick. JAMA 313(12):1249–1255
8. Huttner A, Dayer JA, Yerly S, Combescure C, Auderset F, Desmeules J, Eickmann M, Finckh A, Goncalves AR, Hooper JW et al (2015) The effect of dose on the safety and immunogenicity of the VSV Ebola candidate vaccine: a randomised double-blind, placebo-controlled phase 1/2 trial. Lancet Infect Dis 15(10):1156–1166
9. Henao-Restrepo AM, Longini IM, Egger M, Dean NE, Edmunds WJ, Camacho A, Carroll MW, Doumbia M, Draguez B, Duraffour S et al (2015) Efficacy and effectiveness of an rVSV-vectored vaccine expressing Ebola surface glycoprotein: interim results from the Guinea ring vaccination cluster-randomised trial. Lancet 386(9996):857–866
10. Agnandji ST, Huttner A, Zinser ME, Njuguna P, Dahlke C, Fernandes JF, Yerly S, Dayer JA, Kraehling V, Kasonta R et al (2015) Phase 1 trials of rVSV Ebola vaccine in Africa and Europe—preliminary report. N Engl J Med. doi: 10.1056/NEJMoa1502924
11. Ledgerwood JE, DeZure AD, Stanley DA, Novik L, Enama ME, Berkowitz NM, Hu Z, Joshi G, Ploquin A, Sitar S et al (2014) Chimpanzee adenovirus vector Ebola vaccine—preliminary report. N Engl J Med. doi:10.1056/NEJMoa1410863
12. Blaney JE, Marzi A, Willet M, Papaneri AB, Wirblich C, Feldmann F, Holbrook M, Jahrling P, Feldmann H, Schnell MJ (2013) Antibody quality and protection from lethal Ebola virus challenge in nonhuman primates immunized with rabies virus based bivalent vaccine. PLoS Pathog 9(5):e1003389
13. Ha M, Kim VN (2014) Regulation of microRNA biogenesis. Nat Rev Mol Cell Biol 15(8):509–524
14. Siomi H, Siomi MC (2010) Posttranscriptional regulation of microRNA biogenesis in animals. Mol Cell 38(3):323–332
15. Krol J, Loedige I, Filipowicz W (2010) The widespread regulation of microRNA biogenesis, function and decay. Nat Rev Genet 11(9):597–610
16. Kozomara A, Griffiths-Jones S (2014) miRBase: annotating high confidence microRNAs using deep sequencing data. Nucleic Acids Res 42 (database issue):D68–73
17. Cullen BR (2010) Five questions about viruses and microRNAs. PLoS Pathog 6(2):e1000787
18. Kincaid RP, Sullivan CS (2012) Virus-encoded microRNAs: an overview and a look to the future. PLoS Pathog 8(12):e1003018
19. Rouha H, Thurner C, Mandl CW (2010) Functional microRNA generated from a cytoplasmic RNA virus. Nucleic Acids Res 38(22):8328–8337

20. Kaul D, Ahlawat A, Gupta SD (2009) HIV-1 genome-encoded hiv1-mir-H1 impairs cellular responses to infection. Mol Cell Biochem 323(1–2):143–148
21. Hussain M, Torres S, Schnettler E, Funk A, Grundhoff A, Pijlman GP, Khromykh AA, Asgari S (2012) West Nile virus encodes a microRNA-like small RNA in the 3′ untranslated region which up-regulates GATA4 mRNA and facilitates virus replication in mosquito cells. Nucleic Acids Res 40(5):2210–2223
22. Rosewick N, Momont M, Durkin K, Takeda H, Caiment F, Cleuter Y, Vernin C, Mortreux F, Wattel E, Burny A et al (2013) Deep sequencing reveals abundant noncanonical retroviral microRNAs in B-cell leukemia/lymphoma. Proc Natl Acad Sci USA 110(6):2306–2311
23. Kincaid RP, Burke JM, Sullivan CS (2012) RNA virus microRNA that mimics a B-cell oncomiR. Proc Natl Acad Sci USA 109(8):3077–3082
24. Skalsky RL, Olson KE, Blair CD, Garcia-Blanco MA, Cullen BR (2014) A "microRNA-like" small RNA expressed by Dengue virus? Proc Natl Acad Sci USA 111(23):E2359
25. Hussain M, Asgari S (2014) MicroRNA-like viral small RNA from Dengue virus 2 autoregulates its replication in mosquito cells. Proc Natl Acad Sci USA 111(7):2746–2751
26. Hussain M, Asgari S (2014) Reply to Skalsky et al.: A microRNA-like small RNA from Dengue virus. Proc Natl Acad Sci USA 111(23):E2360
27. Shi J, Duan Z, Sun J, Wu M, Wang B, Zhang J, Wang H, Hu N, Hu Y (2014) Identification and validation of a novel microRNA-like molecule derived from a cytoplasmic RNA virus antigenome by bioinformatics and experimental approaches. Virol J 11:121
28. Teng Y, Wang Y, Zhang X, Liu W, Fan H, Yao H, Lin B, Zhu P, Yuan W, Tong Y et al (2015) Systematic genome-wide screening and prediction of microRNAs in EBOV during the 2014 Ebola-virus outbreak. Sci Rep 5:9912
29. Liang H, Zhou Z, Zhang S, Zen K, Chen X, Zhang C (2014) Identification of Ebola virus microRNAs and their putative pathological function. Sci China Life Sci 57(10):973–981
30. Tempel S, Tahi F (2012) A fast ab initio method for predicting miRNA precursors in genomes. Nucleic Acids Res 40(11):e80
31. Jiang P, Wu H, Wang W, Ma W, Sun X, Lu Z (2007) MiPred: classification of real and pseudo microRNA precursors using random forest prediction model with combined features. Nucleic Acids Res (web server issue) 35:W339–344
32. Zhang Y, Yang Y, Zhang H, Jiang X, Xu B, Xue Y, Cao Y, Zhai Q, Zhai Y, Xu M et al (2011) Prediction of novel pre-microRNAs with high accuracy through boosting and SVM. Bioinformatics 27(10):1436–1437
33. Gkirtzou K, Tsamardinos I, Tsakalides P, Poirazi P (2010) MatureBayes: a probabilistic algorithm for identifying the mature miRNA within novel precursors. PLoS One 5(8):e11843
34. Gruber AR, Lorenz R, Bernhart SH, Neubock R, Hofacker IL (2008) The Vienna RNA websuite. Nucleic Acids Res 36 (web server issue):W70–W74
35. Popenda M, Szachniuk M, Antczak M, Purzycka KJ, Lukasiak P, Bartol N, Blazewicz J, Adamiak RW (2012) Automated 3D structure composition for large RNAs. Nucleic Acids Res 40(14):e112
36. Blankenberg D, Von Kuster G, Coraor N, Ananda G, Lazarus R, Mangan M, Nekrutenko A, Taylor J (2010) Galaxy: a web-based genome analysis tool for experimentalists. Curr Protoc Mol Biol 19(10):11–21
37. Giardine B, Riemer C, Hardison RC, Burhans R, Elnitski L, Shah P, Zhang Y, Blankenberg D, Albert I, Taylor J et al (2005) Galaxy: a platform for interactive large-scale genome analysis. Genome Res 15(10):1451–1455
38. Goecks J, Nekrutenko A, Taylor J (2010) Galaxy: a comprehensive approach for supporting accessible, reproducible, and transparent computational research in the life sciences. Genome Biol 11(8):R86
39. Milne I, Bayer M, Cardle L, Shaw P, Stephen G, Wright F, Marshall D (2010) Tablet–next generation sequence assembly visualization. Bioinformatics 26(3):401–402
40. Milne I, Stephen G, Bayer M, Cock PJ, Pritchard L, Cardle L, Shaw PD, Marshall D (2013) Using Tablet for visual exploration of second-generation sequencing data. Brief Bioinform 14(2):193–202
41. Kent WJ, Sugnet CW, Furey TS, Roskin KM, Pringle TH, Zahler AM, Haussler D (2002) The human genome browser at UCSC. Genome Res 12(6):996–1006
42. Lewis BP, Burge CB, Bartel DP (2005) Conserved seed pairing, often flanked by adenosines, indicates that thousands of human genes are microRNA targets. Cell 120(1):15–20
43. Mi H, Muruganujan A, Casagrande JT, Thomas PD (2013) Large-scale gene function analysis with the PANTHER classification system. Nat Protoc 8(8):1551–1566
44. Kamburov A, Pentchev K, Galicka H, Wierling C, Lehrach H, Herwig R (2011) ConsensusPathDB: toward a more complete picture of cell biology. Nucleic Acids Res 39 (Database issue):D712–717
45. Kamburov A, Wierling C, Lehrach H, Herwig R (2009) ConsensusPathDB—a database for integrating human functional interaction networks. Nucleic Acids Res 37 (Database issue):D623–628
46. Chen C, Ridzon DA, Broomer AJ, Zhou Z, Lee DH, Nguyen JT, Barbisin M, Xu NL, Mahuvakar VR, Andersen MR et al (2005) Real-time quantification of microRNAs by stem-loop RT-PCR. Nucleic Acids Res 33(20):e179
47. Gire SK, Goba A, Andersen KG, Sealfon RS, Park DJ, Kanneh L, Jalloh S, Momoh M, Fullah M, Dudas G et al (2014) Genomic surveillance elucidates Ebola virus origin and transmission during the 2014 outbreak. Science 345(6202):1369–1372
48. Mateo M, Reid SP, Leung LW, Basler CF, Volchkov VE (2010) Ebolavirus VP24 binding to karyopherins is required for inhibition of interferon signaling. J Virol 84(2):1169–1175
49. Reid SP, Leung LW, Hartman AL, Martinez O, Shaw ML, Carbonnelle C, Volchkov VE, Nichol ST, Basler CF (2006) Ebola virus VP24 binds karyopherin alpha1 and blocks STAT1 nuclear accumulation. J Virol 80(11):5156–5167
50. Reid SP, Valmas C, Martinez O, Sanchez FM, Basler CF (2007) Ebola virus VP24 proteins inhibit the interaction of NPI-1 subfamily karyopherin alpha proteins with activated STAT1. J Virol 81(24):13469–13477
51. Shabman RS, Gulcicek EE, Stone KL, Basler CF (2011) The Ebola virus VP24 protein prevents hnRNP C1/C2 binding to karyopherin alpha1 and partially alters its nuclear import. J Infect Dis 204[Suppl 3]:S904–910
52. Yang CY, Kuo TH, Ting LP (2006) Human hepatitis B viral e antigen interacts with cellular interleukin-1 receptor accessory protein and triggers interleukin-1 response. J Biol Chem 281(45):34525–34536
53. Cenciarelli O, Pietropaoli S, Malizia A, Carestia M, D'Amico F, Sassolini A, Di Giovanni D, Rea S, Gabbarini V, Tamburrini A et al (2015) Ebola virus disease 2013-2014 outbreak in west Africa: an analysis of the epidemic spread and response. Int J Microbiol 2015:769121
54. Feldmann H, Geisbert TW (2011) Ebola haemorrhagic fever. Lancet 377(9768):849–862
55. Yen B, Mulder LC, Martinez O, Basler CF (2014) Molecular basis for ebolavirus VP35 suppression of human dendritic cell maturation. J Virol 88(21):12500–12510
56. Kuhn JH (2008) Filoviruses. A compendium of 40 years of epidemiological, clinical, and laboratory studies. Arch Virol Suppl 20:13–360

57. Weik M, Modrof J, Klenk HD, Becker S, Muhlberger E (2002) Ebola virus VP30-mediated transcription is regulated by RNA secondary structure formation. J Virol 76(17):8532–8539
58. Martinez O, Ndungo E, Tantral L, Miller EH, Leung LW, Chandran K, Basler CF (2013) A mutation in the Ebola virus envelope glycoprotein restricts viral entry in a host species- and cell-type-specific manner. J Virol 87(6):3324–3334
59. Lubaki NM, Ilinykh P, Pietzsch C, Tigabu B, Freiberg AN, Koup RA, Bukreyev A (2013) The lack of maturation of Ebola virus-infected dendritic cells results from the cooperative effect of at least two viral domains. J Virol 87(13):7471–7485
60. Xu W, Edwards MR, Borek DM, Feagins AR, Mittal A, Alinger JB, Berry KN, Yen B, Hamilton J, Brett TJ et al (2014) Ebola virus VP24 targets a unique NLS binding site on karyopherin alpha 5 to selectively compete with nuclear import of phosphorylated STAT1. Cell Host Microbe 16(2):187–200
61. Gabriel G, Feldmann F, Reimer R, Thiele S, Fischer M, Hartmann E, Bader M, Ebihara H, Hoenen T, Feldmann H (2015) Importin-alpha7 is involved in the formation of Ebola virus inclusion bodies but is not essential for pathogenicity in mice. J Infect Dis 212[Suppl 2]:S316–321
62. George J, Lewis MG, Renne R, Mattapallil JJ (2015) Suppression of transforming growth factor beta receptor 2 and Smad5 is associated with high levels of microRNA miR-155 in the oral mucosa during chronic simian immunodeficiency virus infection. J Virol 89(5):2972–2978
63. Zhao Y, Xu H, Yao Y, Smith LP, Kgosana L, Green J, Petherbridge L, Baigent SJ, Nair V (2011) Critical role of the virus-encoded microRNA-155 ortholog in the induction of Marek's disease lymphomas. PLoS Pathog 7(2):e1001305
64. Yin Q, Wang X, Fewell C, Cameron J, Zhu H, Baddoo M, Lin Z, Flemington EK (2010) MicroRNA miR-155 inhibits bone morphogenetic protein (BMP) signaling and BMP-mediated Epstein–Barr virus reactivation. J Virol 84(13):6318–6327
65. Lu F, Weidmer A, Liu CG, Volinia S, Croce CM, Lieberman PM (2008) Epstein–Barr virus-induced miR-155 attenuates NF-kappaB signaling and stabilizes latent virus persistence. J Virol 82(21):10436–10443
66. Gatto G, Rossi A, Rossi D, Kroening S, Bonatti S, Mallardo M (2008) Epstein-Barr virus latent membrane protein 1 trans-activates miR-155 transcription through the NF-kappaB pathway. Nucleic Acids Res 36(20):6608–6619
67. Skalsky RL, Samols MA, Plaisance KB, Boss IW, Riva A, Lopez MC, Baker HV, Renne R (2007) Kaposi's sarcoma-associated herpesvirus encodes an ortholog of miR-155. J Virol 81(23):12836–12845
68. Chi JQ, Teng M, Yu ZH, Xu H, Su JW, Zhao P, Xing GX, Liang HD, Deng RG, Qu LH et al (2015) Marek's disease virus-encoded analog of microRNA-155 activates the oncogene c-Myc by targeting LTBP1 and suppressing the TGF-beta signaling pathway. Virology 476:72–84
69. Morgan R, Anderson A, Bernberg E, Kamboj S, Huang E, Lagasse G, Isaacs G, Parcells M, Meyers BC, Green PJ et al (2008) Sequence conservation and differential expression of Marek's disease virus microRNAs. J Virol 82(24):12213–12220
70. Yu ZH, Teng M, Sun AJ, Yu LL, Hu B, Qu LH, Ding K, Cheng XC, Liu JX, Cui ZZ et al (2014) Virus-encoded miR-155 ortholog is an important potential regulator but not essential for the development of lymphomas induced by very virulent Marek's disease virus. Virology 448:55–64
71. Wang P, Hou J, Lin L, Wang C, Liu X, Li D, Ma F, Wang Z, Cao X (2010) Inducible microRNA-155 feedback promotes type I IFN signaling in antiviral innate immunity by targeting suppressor of cytokine signaling 1. J Immunol 185(10):6226–6233
72. Hu X, Ye J, Qin A, Zou H, Shao H, Qian K (2015) Both microRNA-155 and virus-encoded MiR-155 ortholog regulate TLR3 expression. PLoS One 10(5):e0126012